

(a) $\Psi=30^\circ$

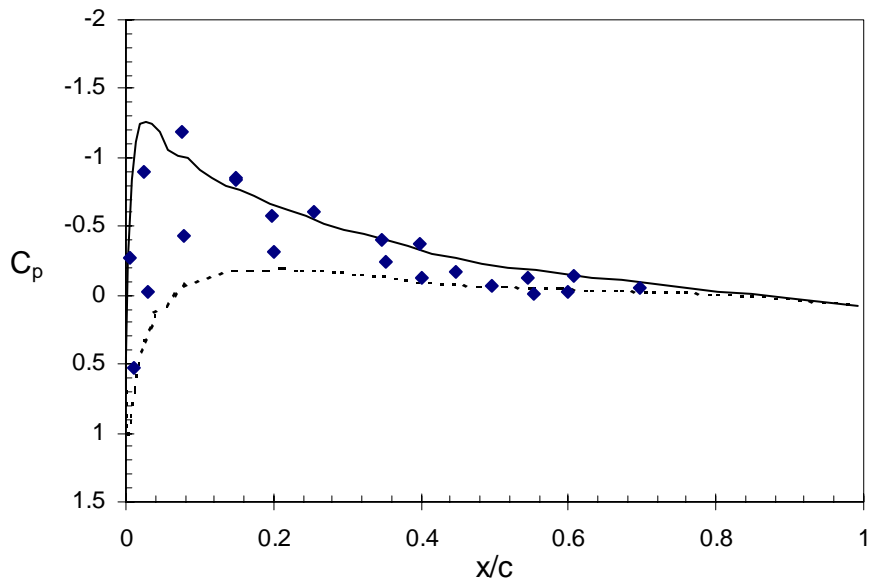
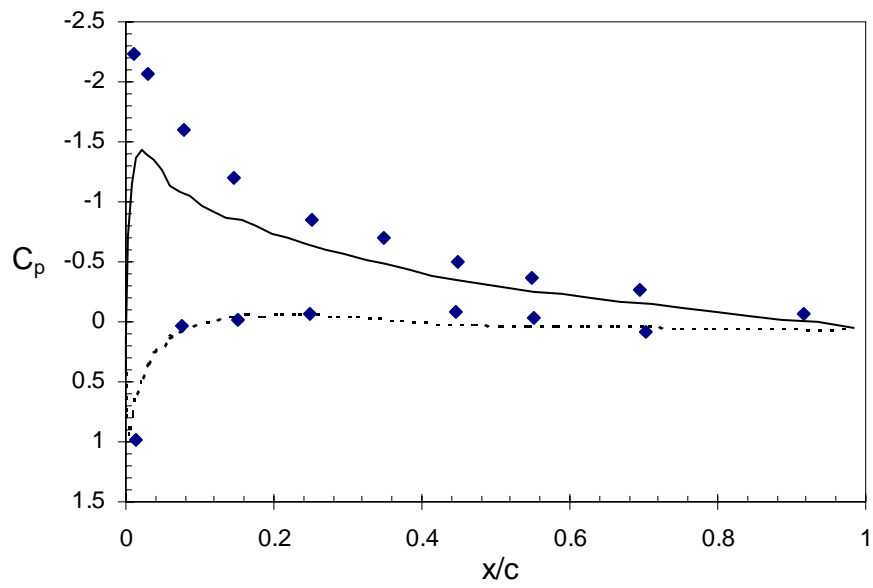
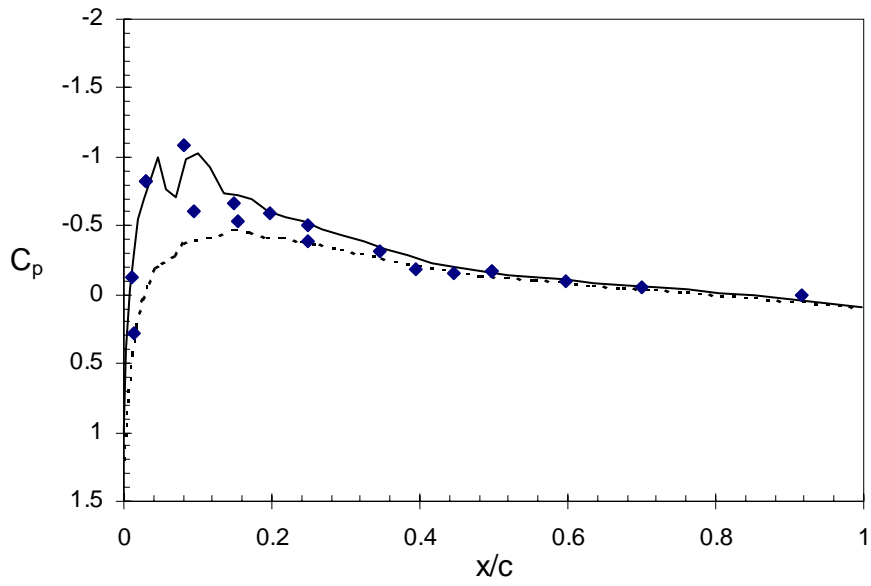


Figure 5.1: Pressure Coefficients for the AH-1G Rotor at $r/R=0.60$



(c) $\Psi=180^\circ$

Figure 5.1: Pressure Coefficients for the AH-1G Rotor at $r/R=0.60$



(a) $\Psi=75^\circ$

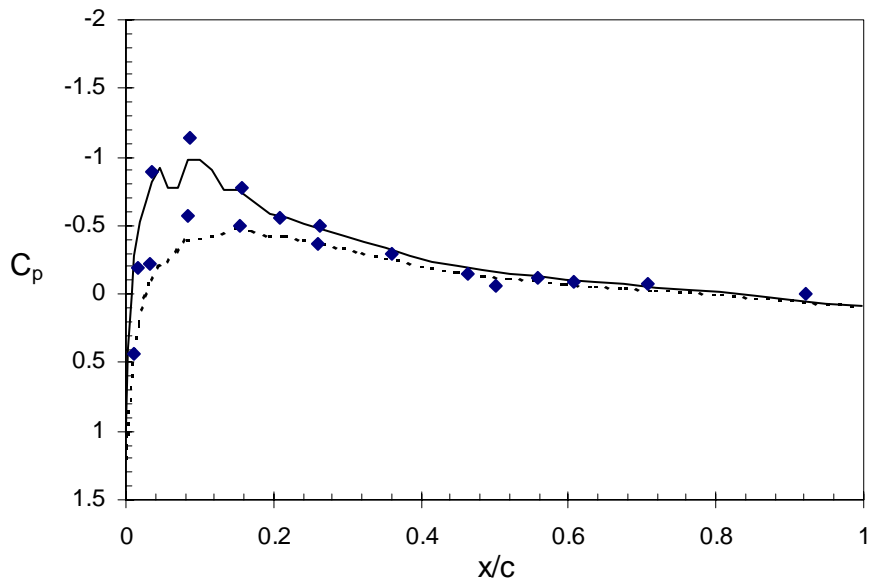
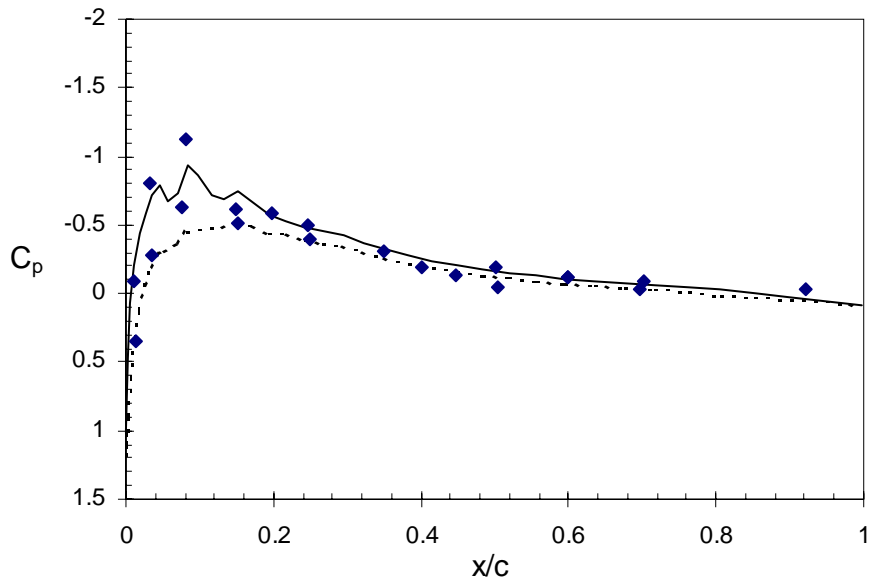


Figure 5.2: Pressure Coefficients for the AH-1G Rotor at $r/R=0.91$



(c) $\Psi=105^\circ$

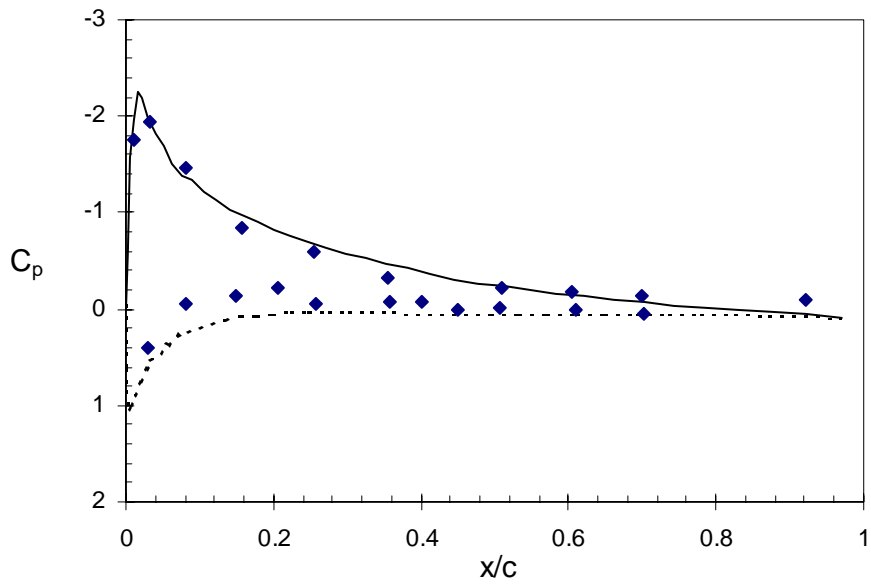
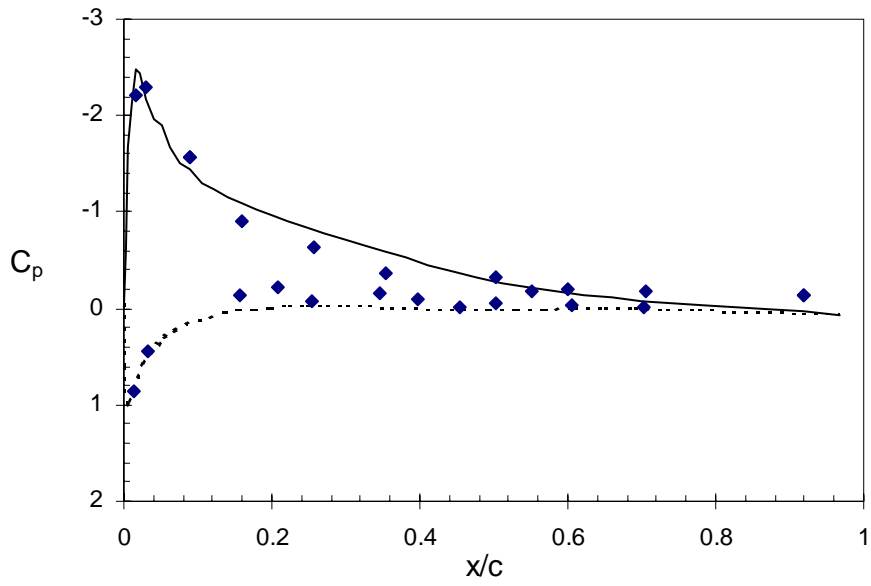


Figure 5.2: Pressure Coefficients for the AH-1G Rotor at $r/R=0.91$



(e) $\Psi=285^\circ$

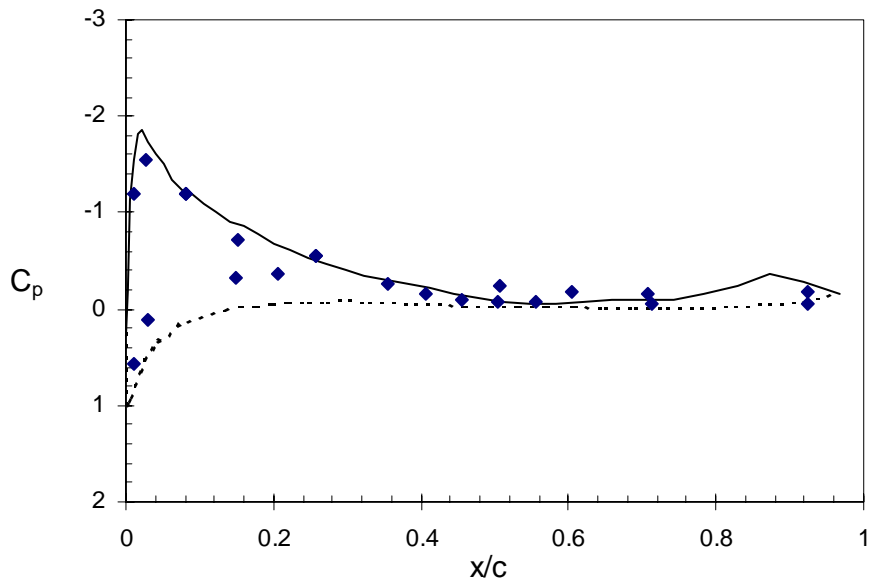
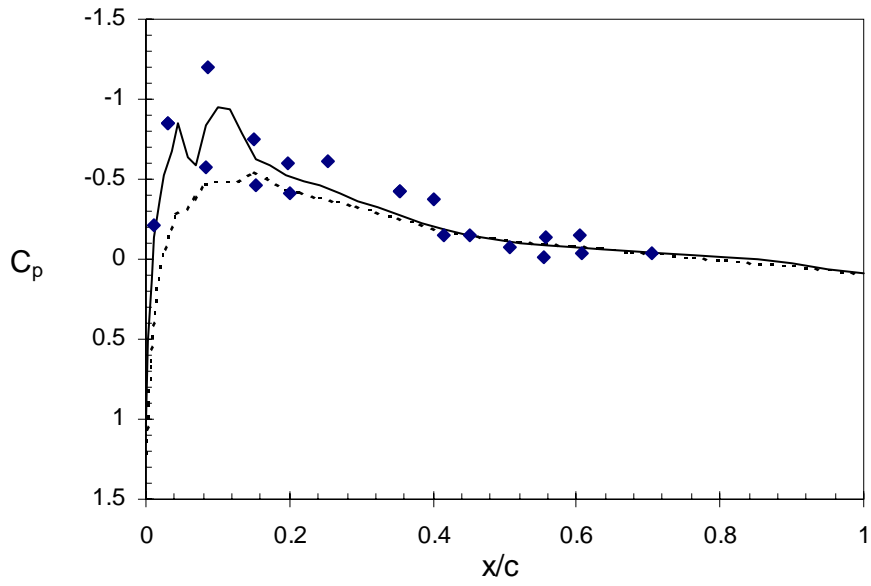


Figure 5.2: Pressure Coefficients for the AH-1G Rotor at $r/R=0.91$



(a) $\Psi=75^\circ$

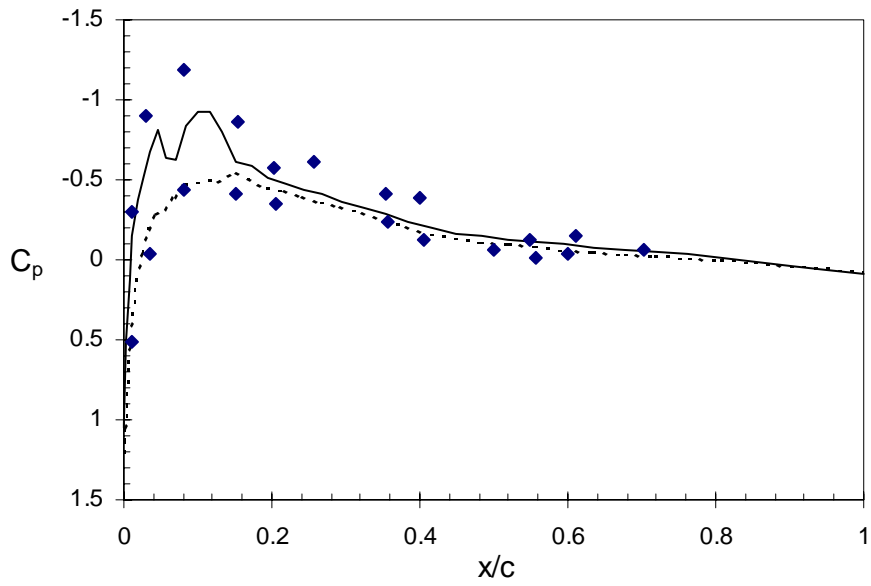
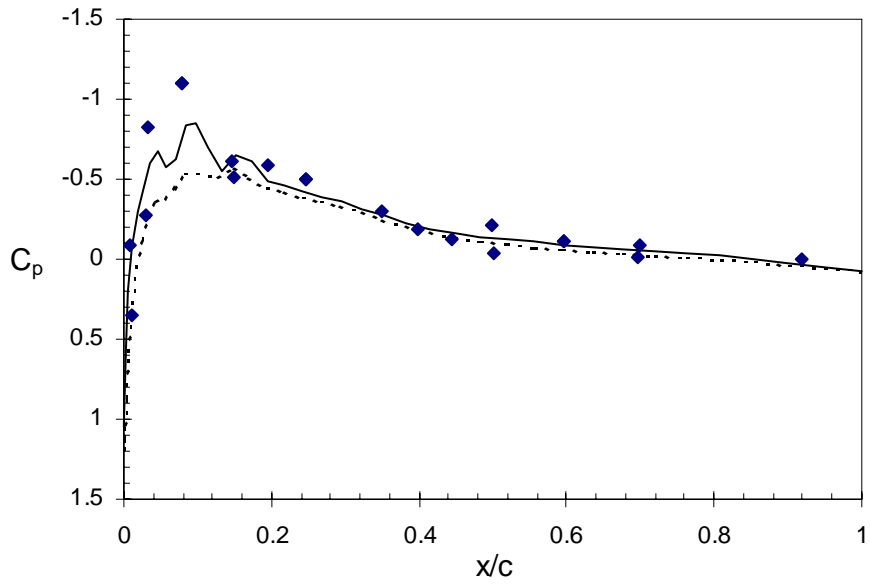


Figure 5.3: Pressure Coefficients for the AH-1G Rotor at $r/R=0.97$



(c) $\Psi=105^\circ$

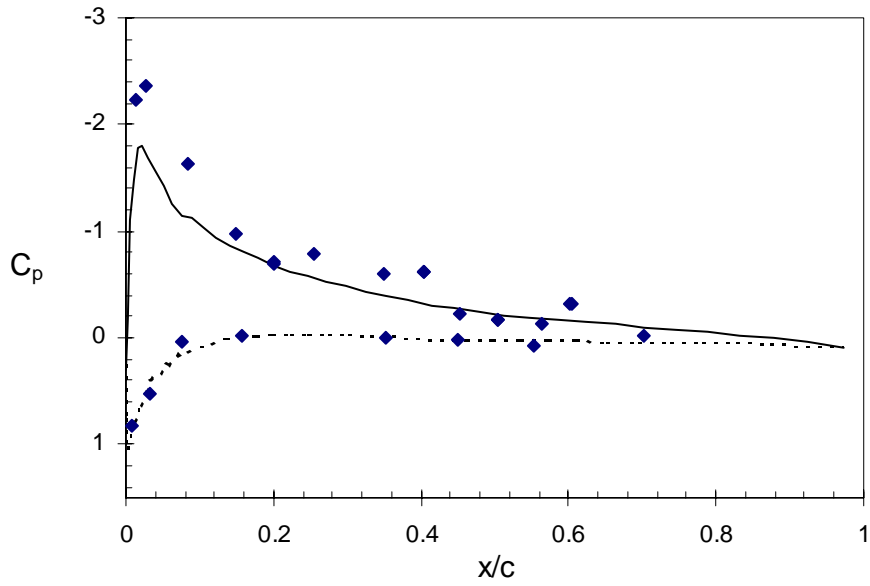


Figure 5.3: Pressure Coefficients for the AH-1G Rotor at $r/R=0.97$

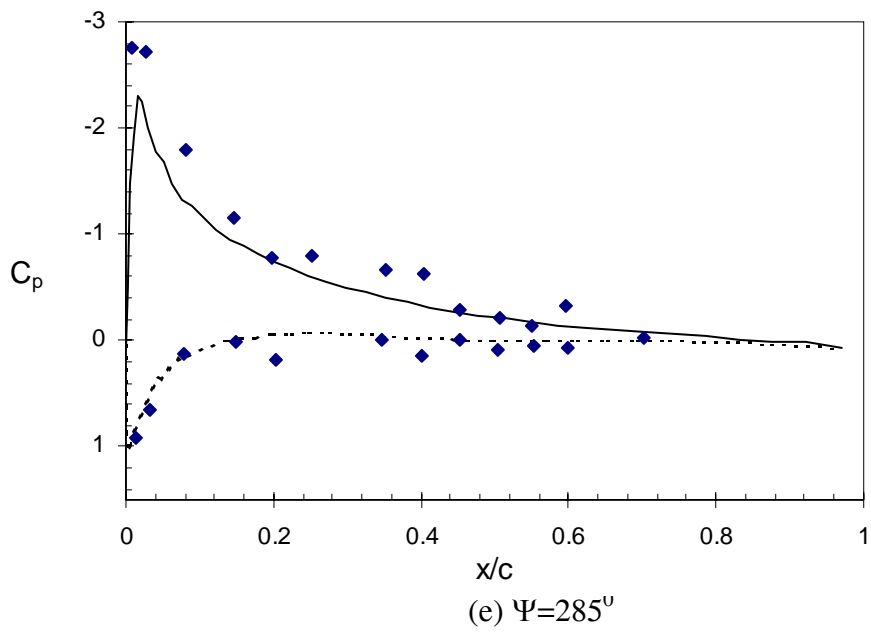
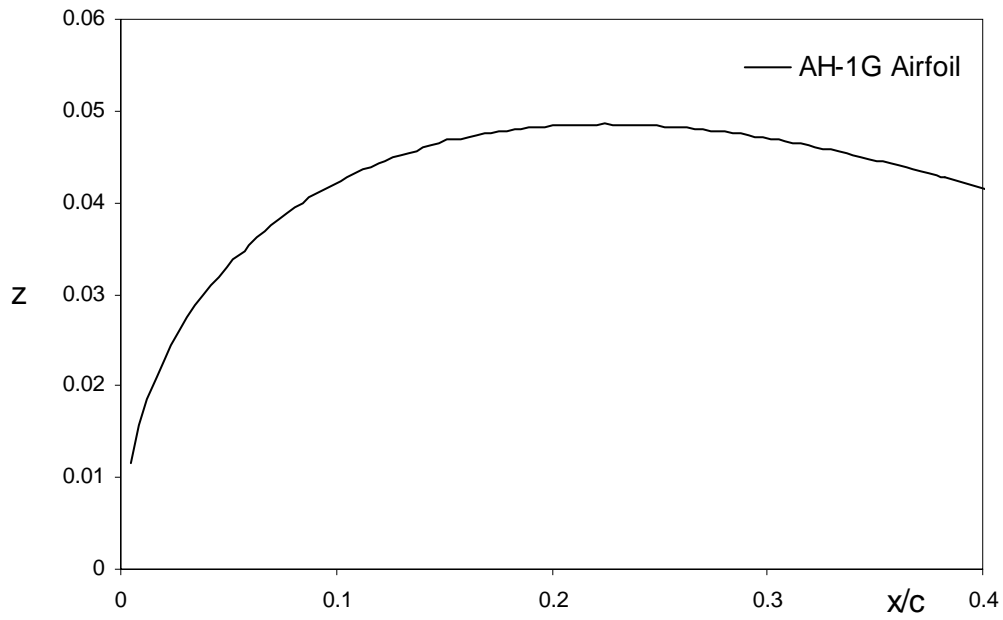
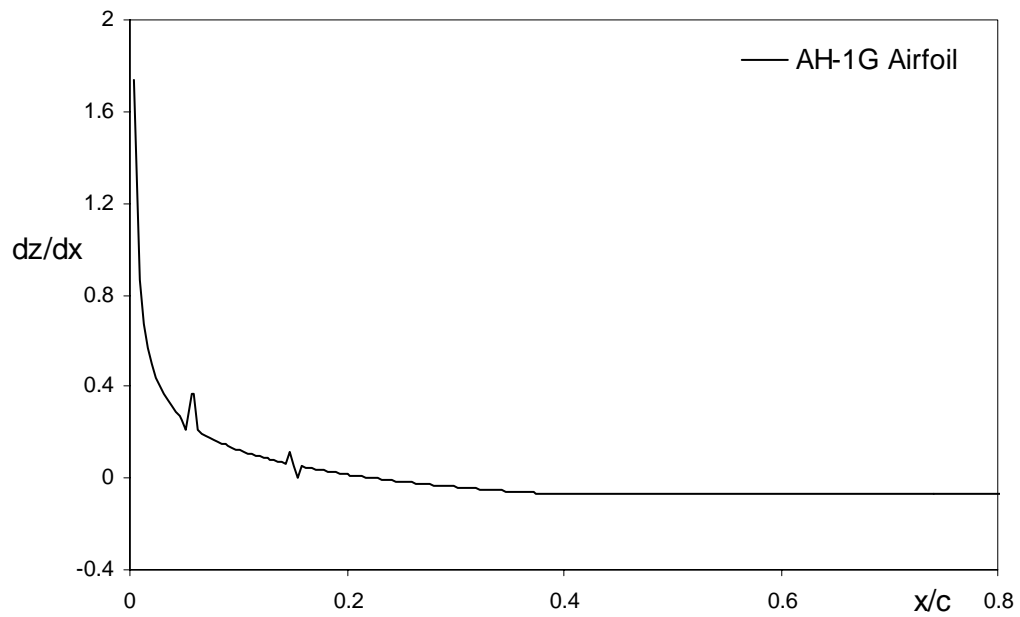


Figure 5.3: Pressure Coefficients for the AH-1G Rotor at $r/R=0.97$



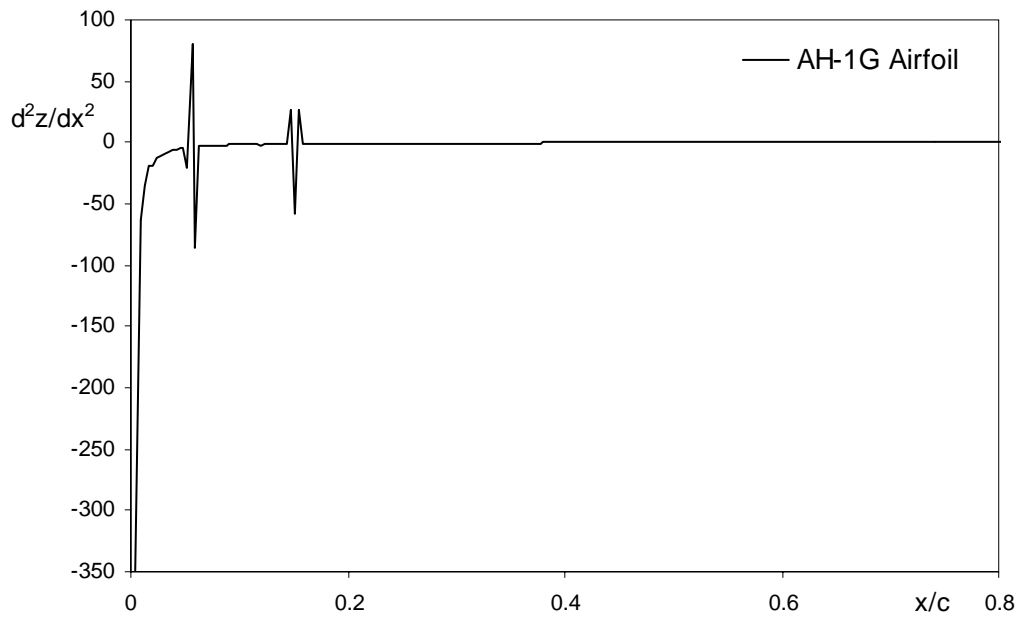
(a) airfoil geometry



(b) first derivative of airfoil geometry

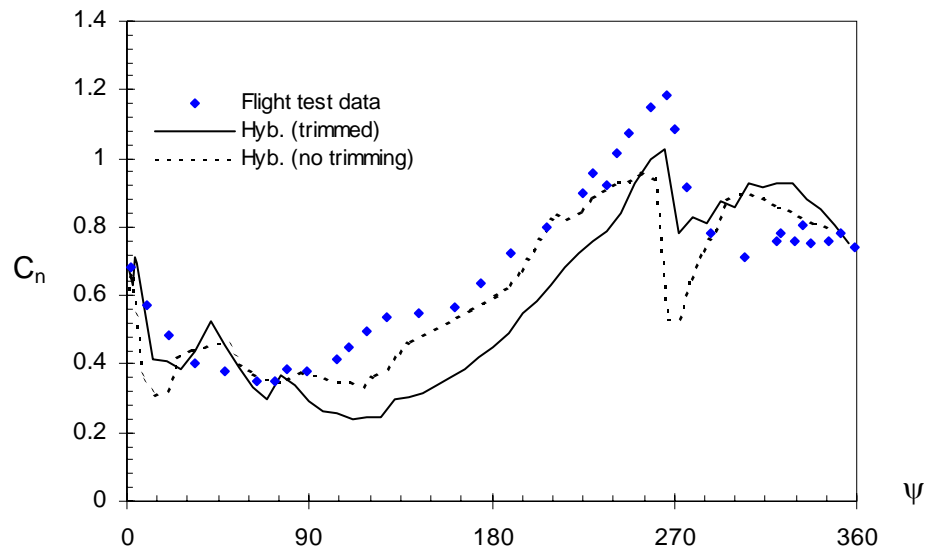
Figure 5.4: The Airfoil Surface Coordinates, Slopes and Curvatures for the

AH-1G Rotor



(c) second derivative of airfoil geometry

Figure 5.4: The Airfoil Surface Coordinates, Slopes and Curvatures for the AH-1G Rotor



(a) $r/R=60\%$

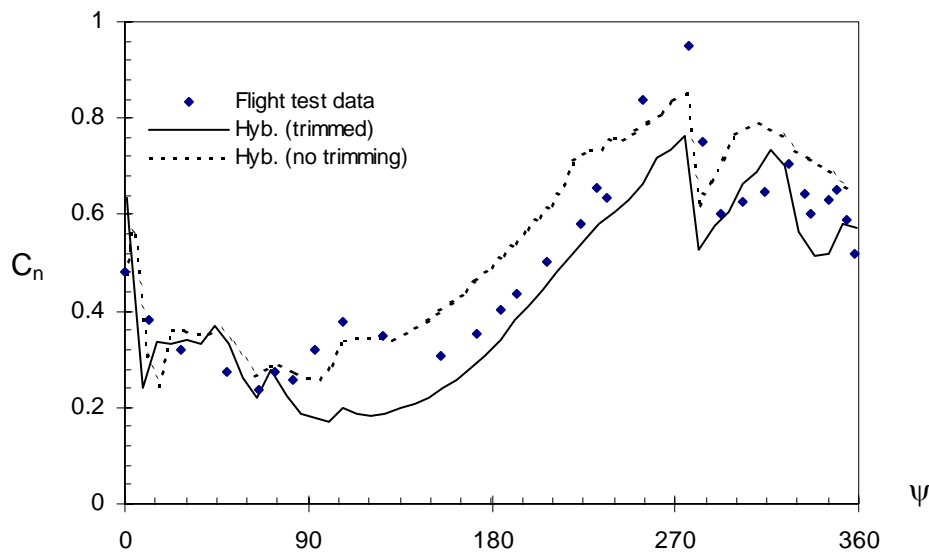
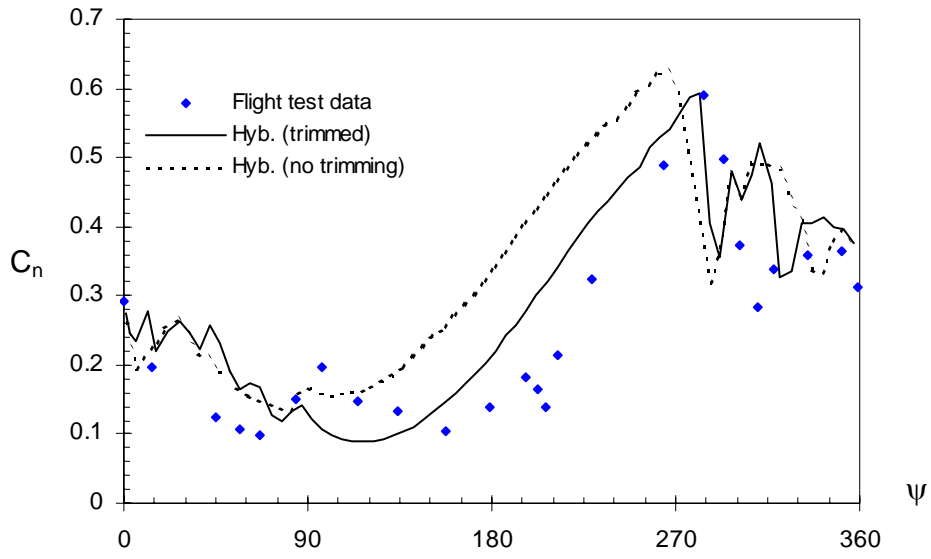


Figure 5.5: Sectional Normal Force Coefficient for the AH-1G Rotor



(c) $r/R=91\%$

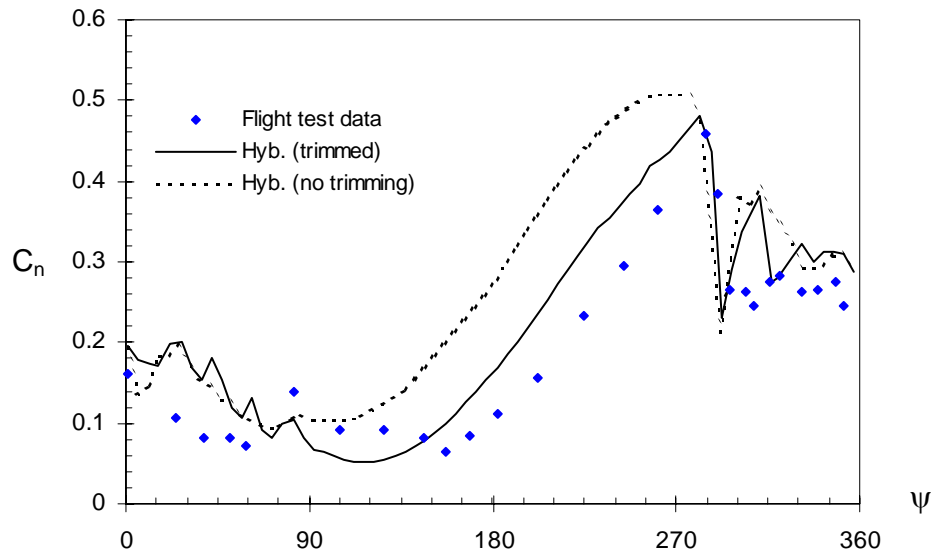
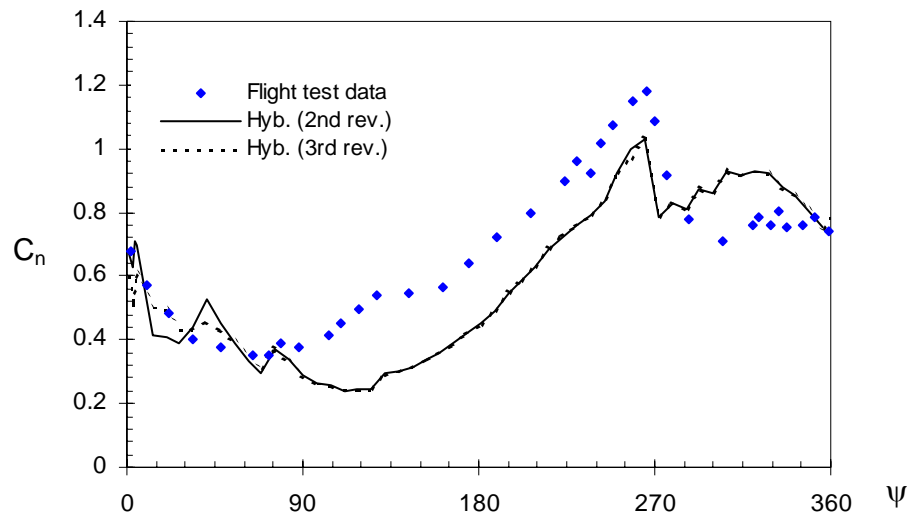
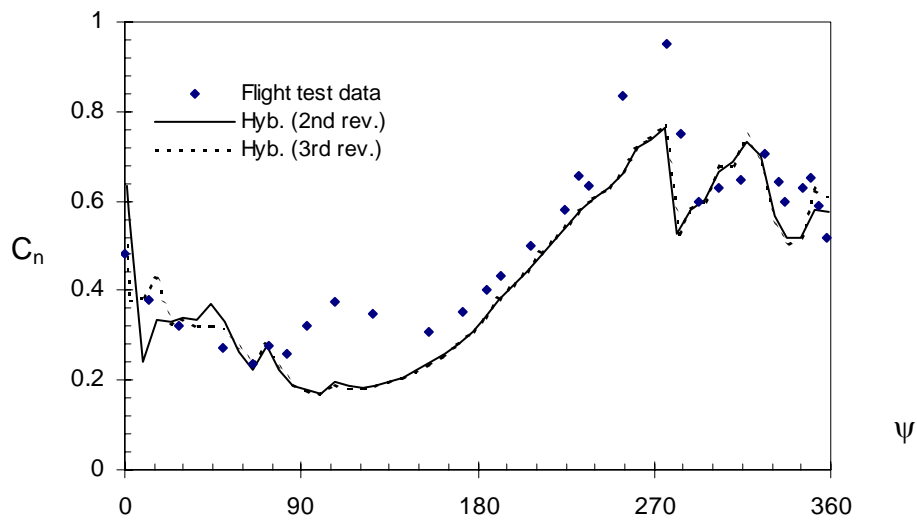


Figure 5.5: Sectional Normal Force Coefficient for the AH-1G Rotor



(a) $r/R=60\%$



(b) $r/R=75\%$

Figure 5.6: Variation of Sectional Normal Force Coefficients from one Revolution to the Next

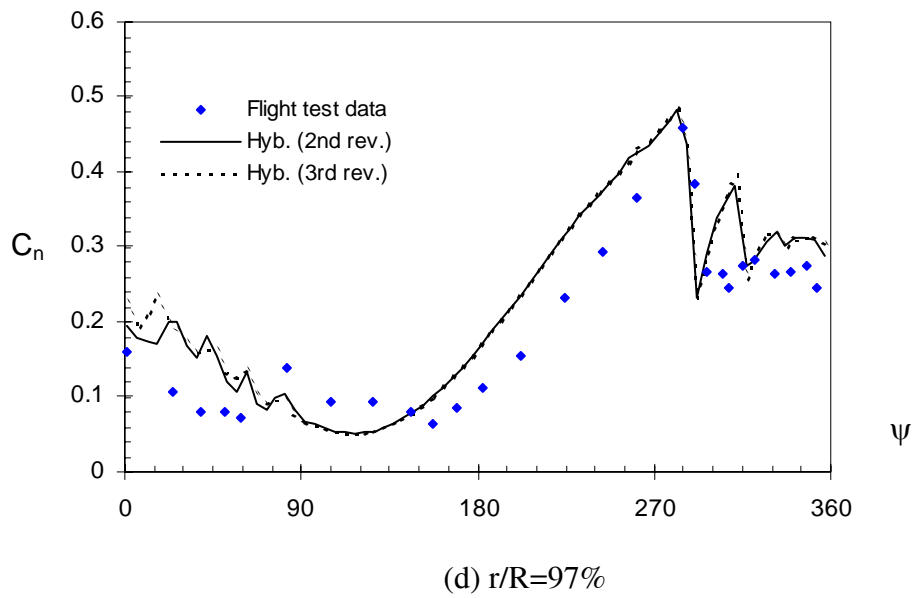
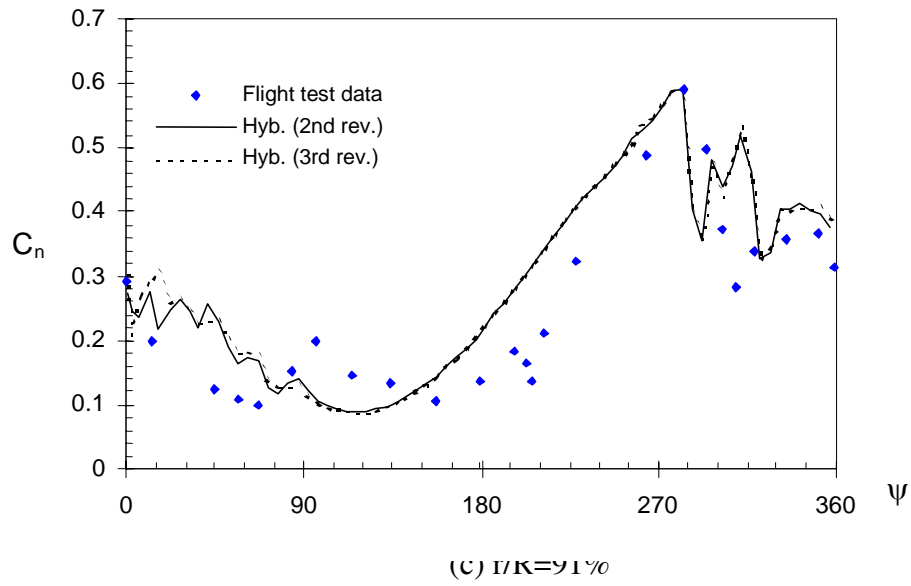


Figure 5.6: Variation of Sectional Normal Force Coefficients from one Revolution to the Next

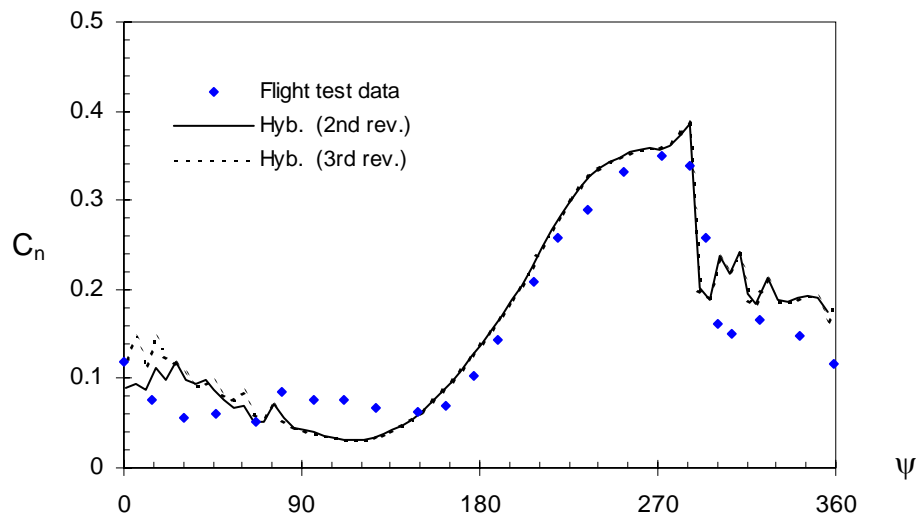
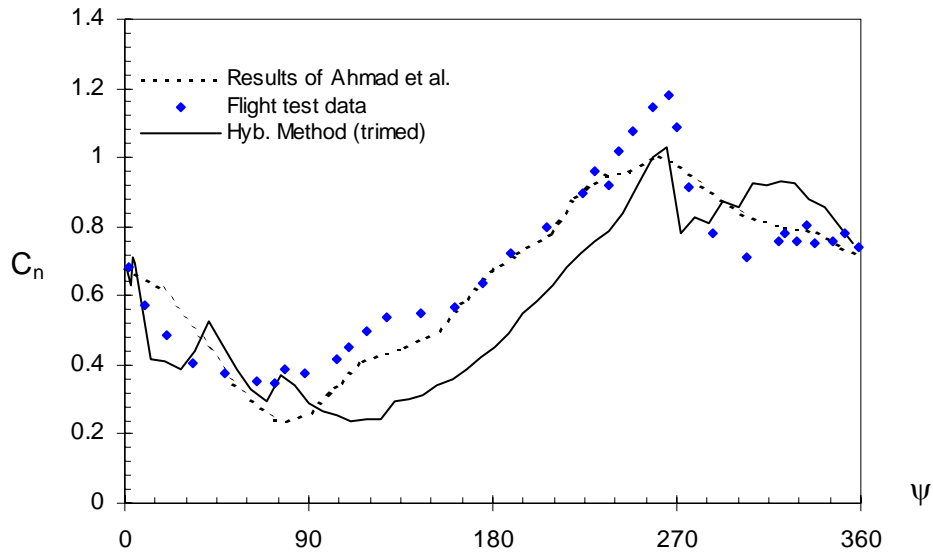


Figure 5.6: Variation of Sectional Normal Force Coefficients from one Revolution to the Next



(a) $r/R=60\%$

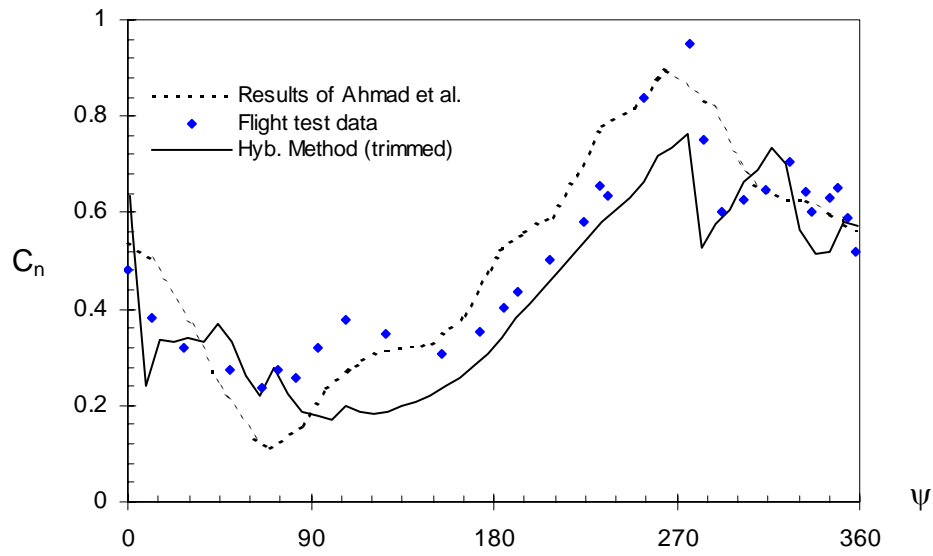
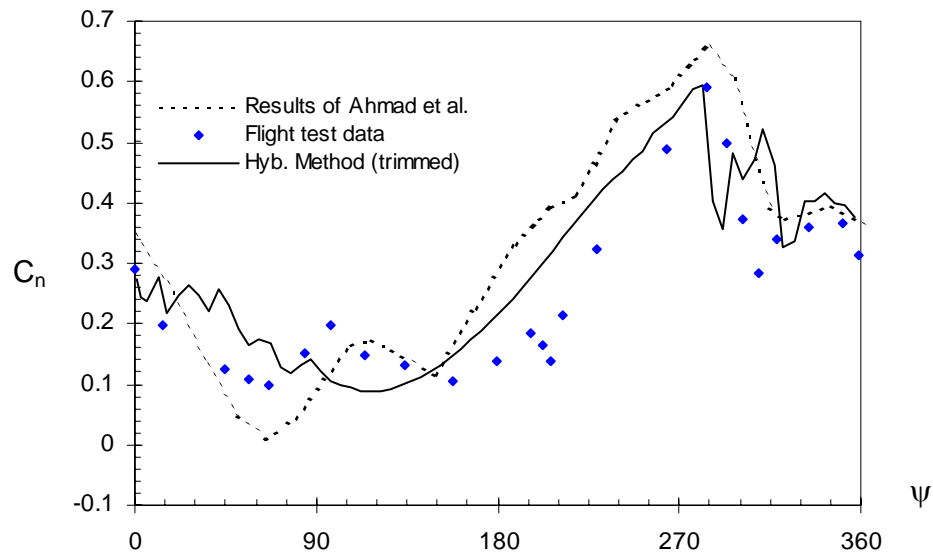


Figure 5.7: Sectional Normal Force Coefficients Compared with Other Calculations



(c) $r/R=91\%$

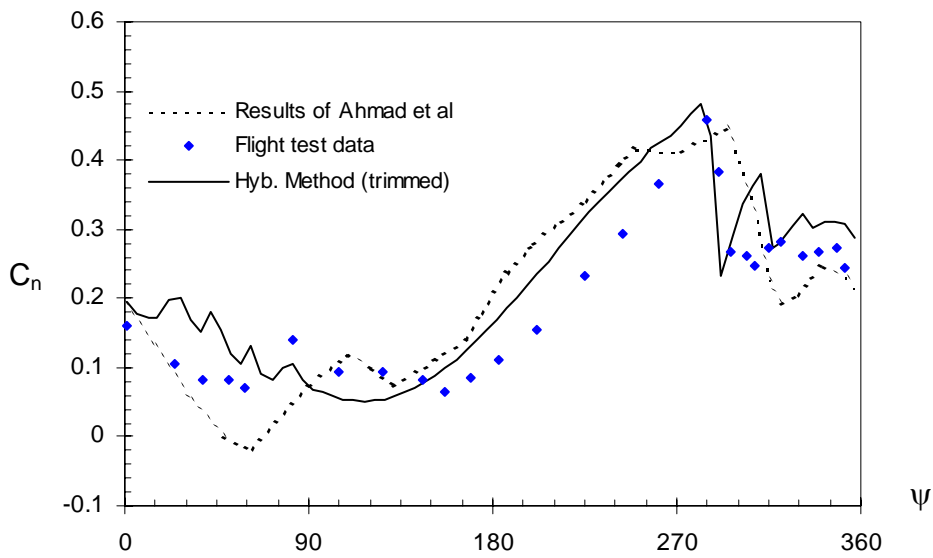
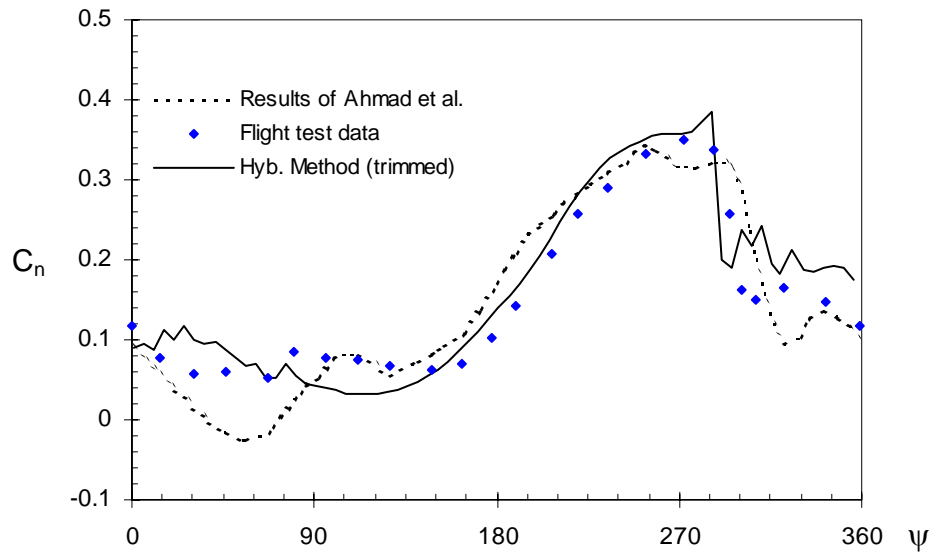
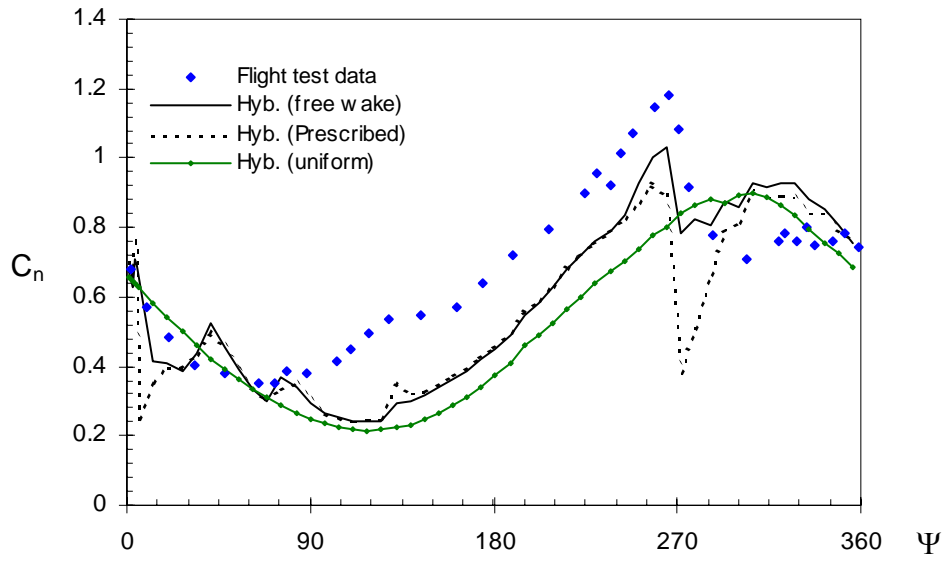


Figure 5.7: Sectional Normal Force Coefficients Compared with Other Calculations



(e) $r/R=99\%$

Figure 5.7: Sectional Normal Force Coefficients Compared with Other Calculations



(a) $r/R=60\%$

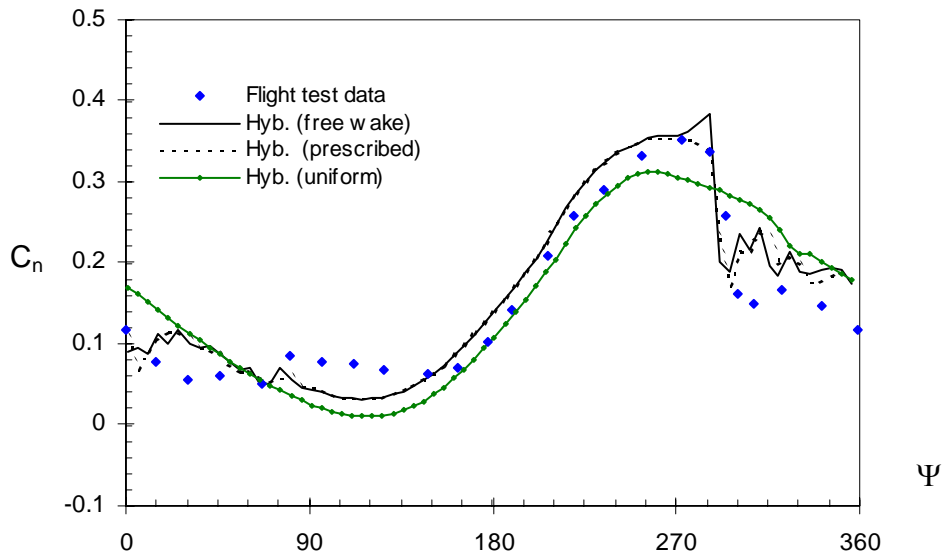
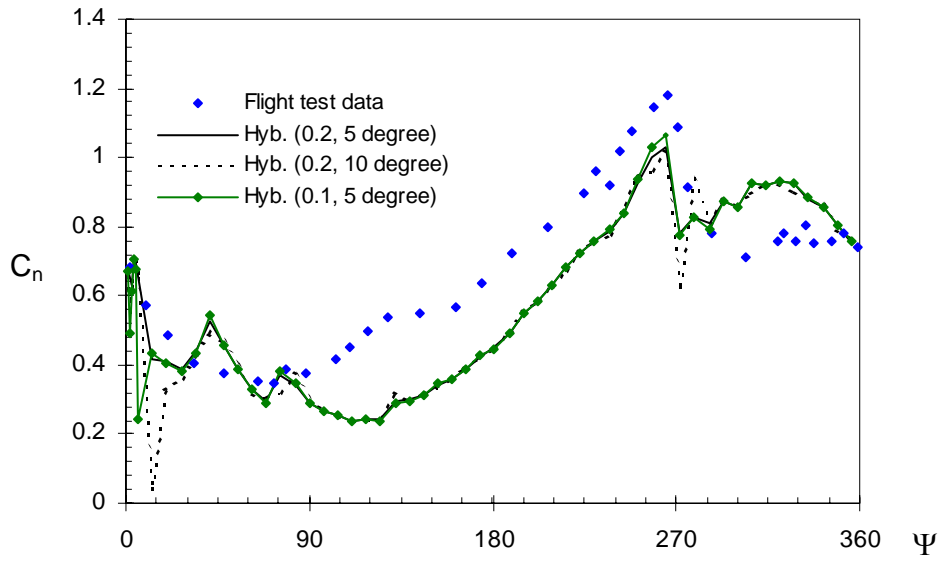
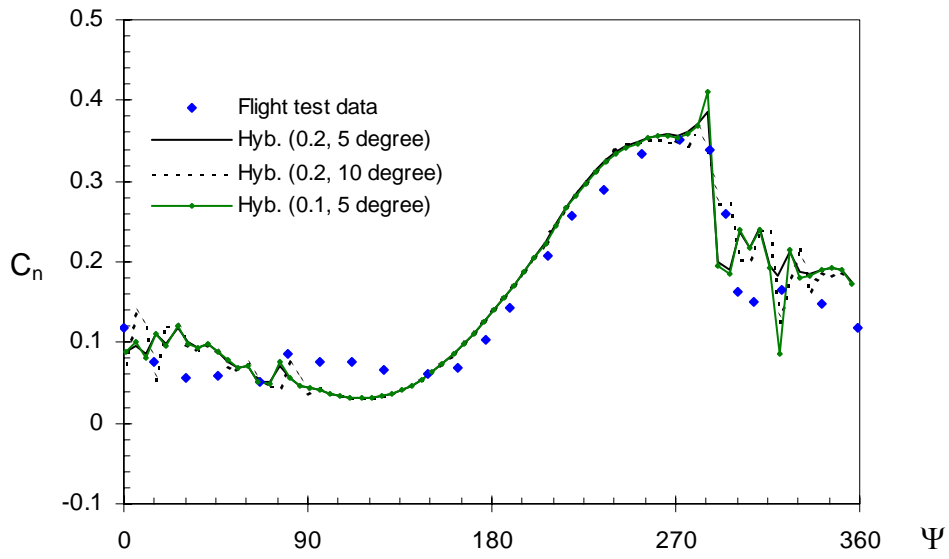


Figure 5.8: Effects of Wake Model on the Sectional Normal Force Coefficients



(a) $r/R=60\%$



(b) $r/R=99\%$

Figure 5.9: Sectional Normal Force Coefficients Computed using the Free Wake Model

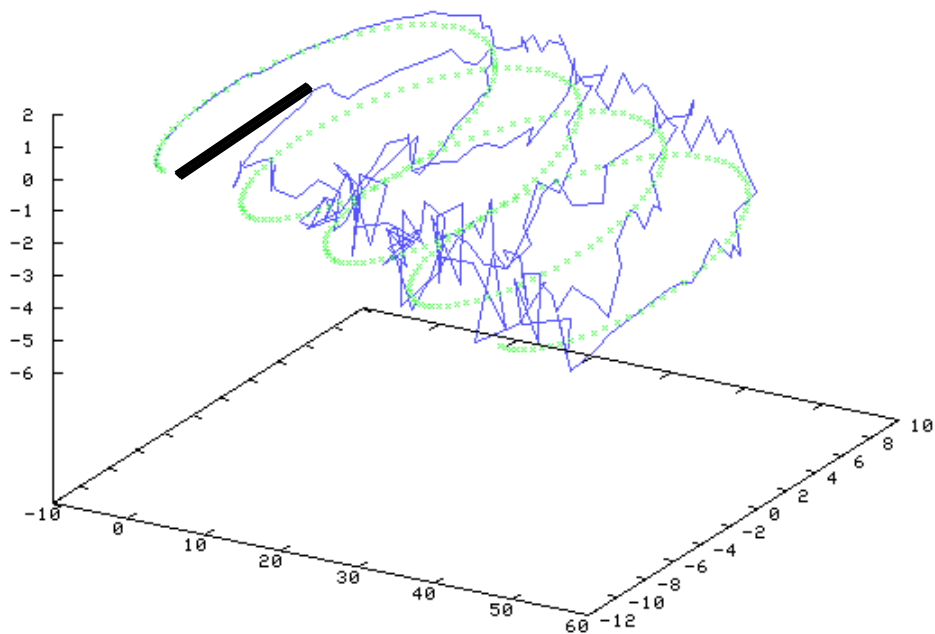
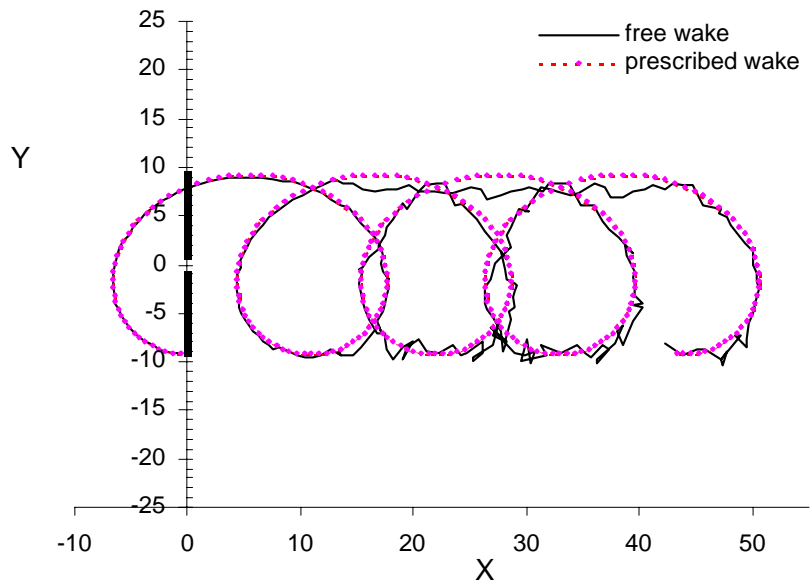


Figure 5.10: Three Views of Wake Shed from Blade at $\Psi=270^\circ$

(solid line for free wake, dash line for prescribed wake)



(b) Plan view

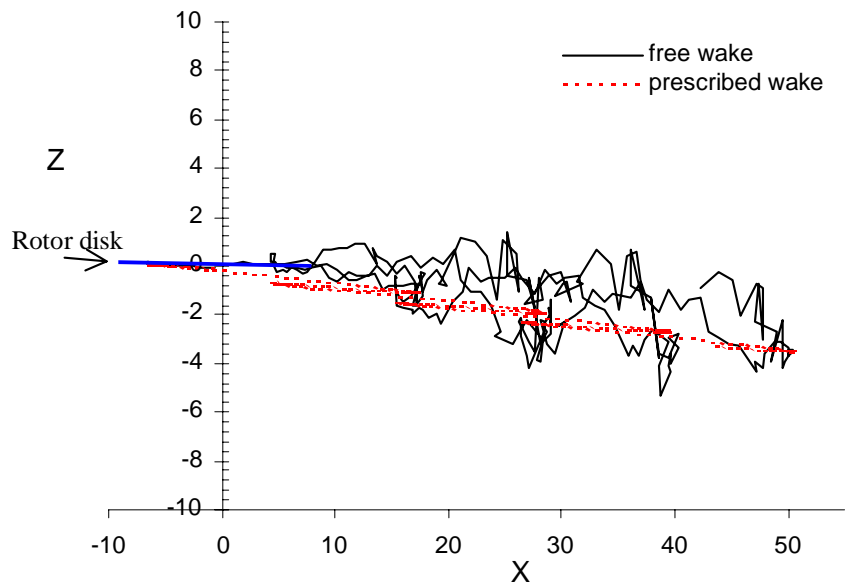
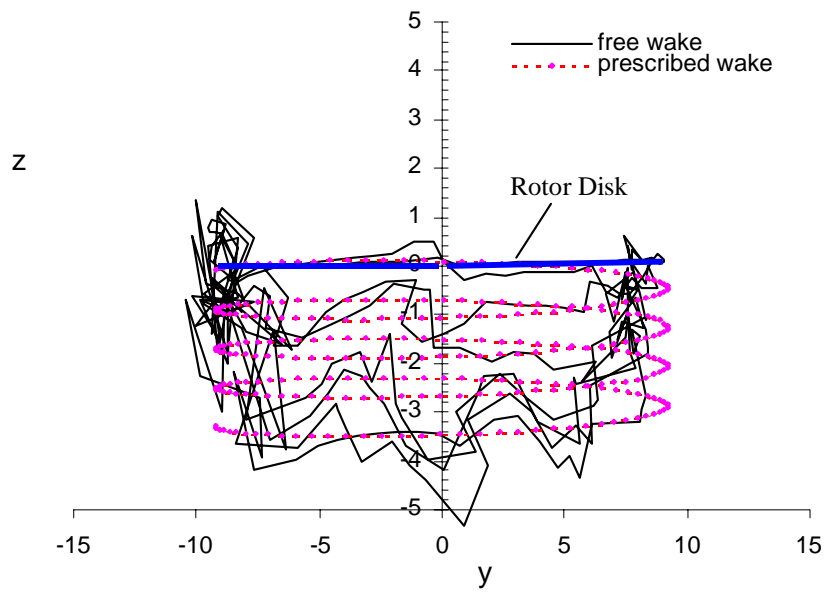


Figure 5.10: Three Views of Wake Shed from Blade at $\Psi=270^0$
(solid line for free wake, dash line for prescribed wake)



(d) Rear view

Figure 5.10: Three Views of Wake Shed from Blade at $\Psi=270^0$

(solid line for free wake, dash line for prescribed wake)

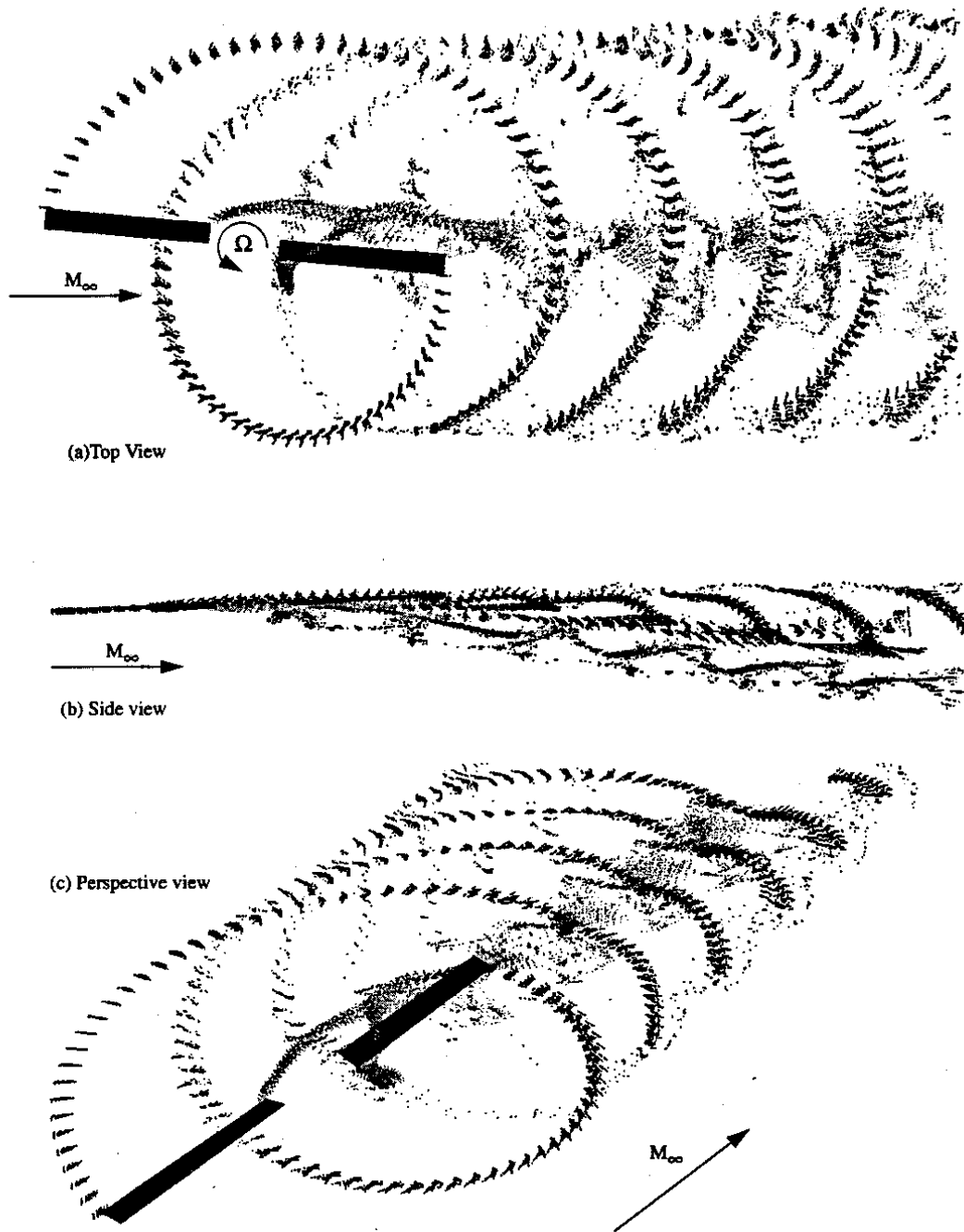
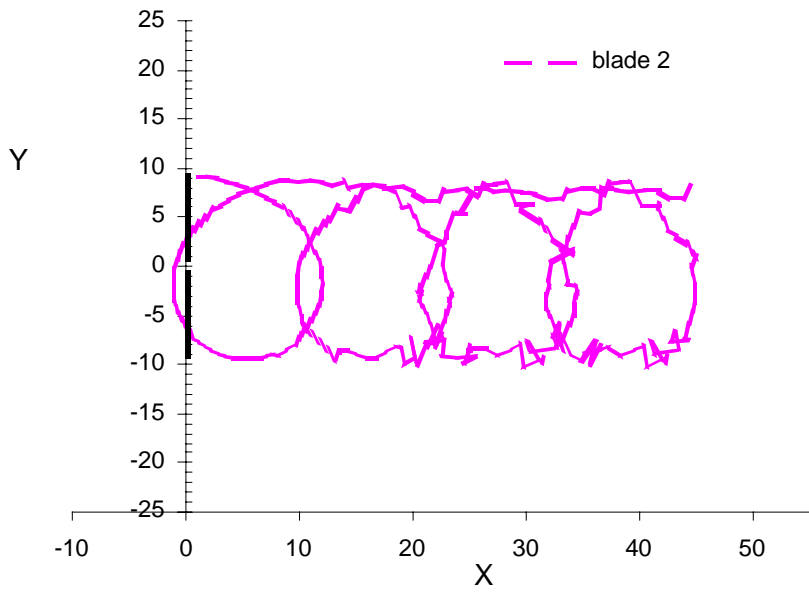


Figure 5.11: Streakline Visualization of the Wake

(reproduced from Ahmad and Duque [58])



(a) free wake

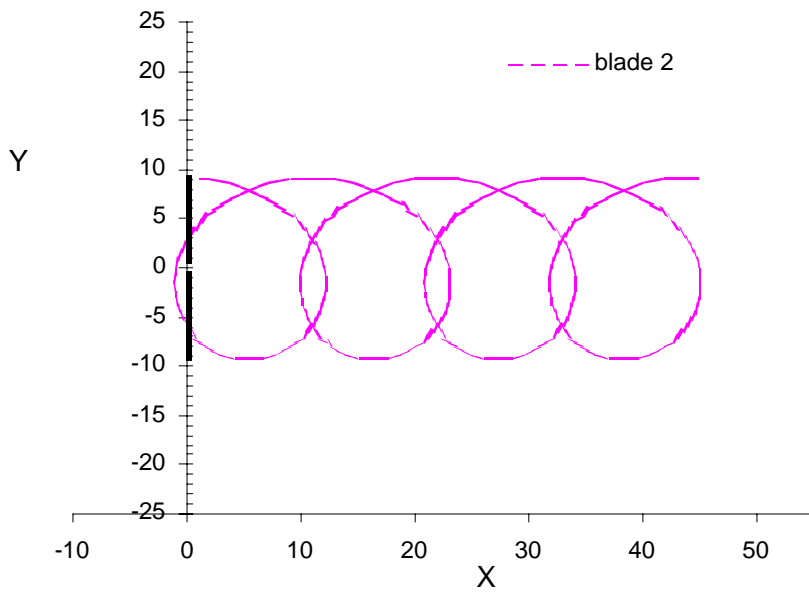


Figure 5.12: PlanView of Wake Shed from the Two Blades with Reference Blade at $\Psi=270^0$

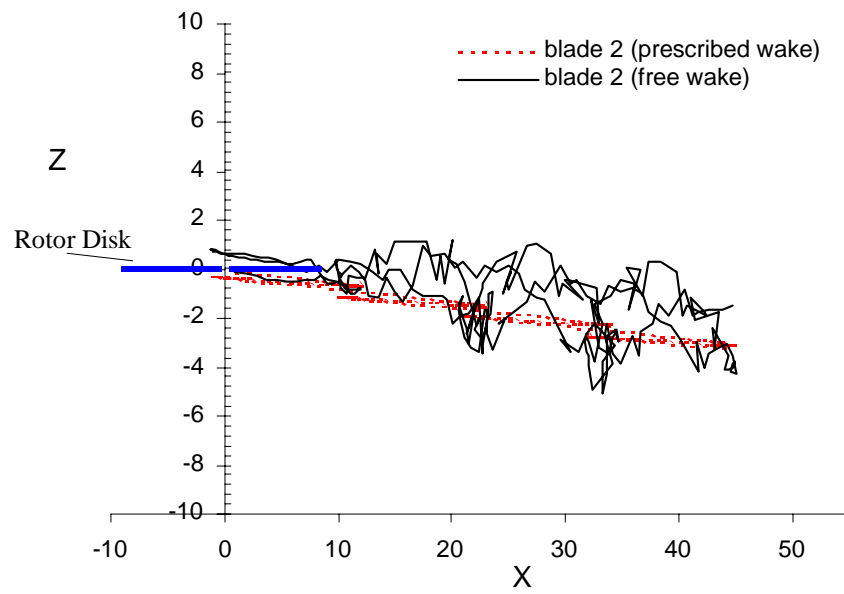


Figure 5.13: Side View of Wake Shed from the Second Blade with Reference
Blade at $\Psi=270^{\circ}$

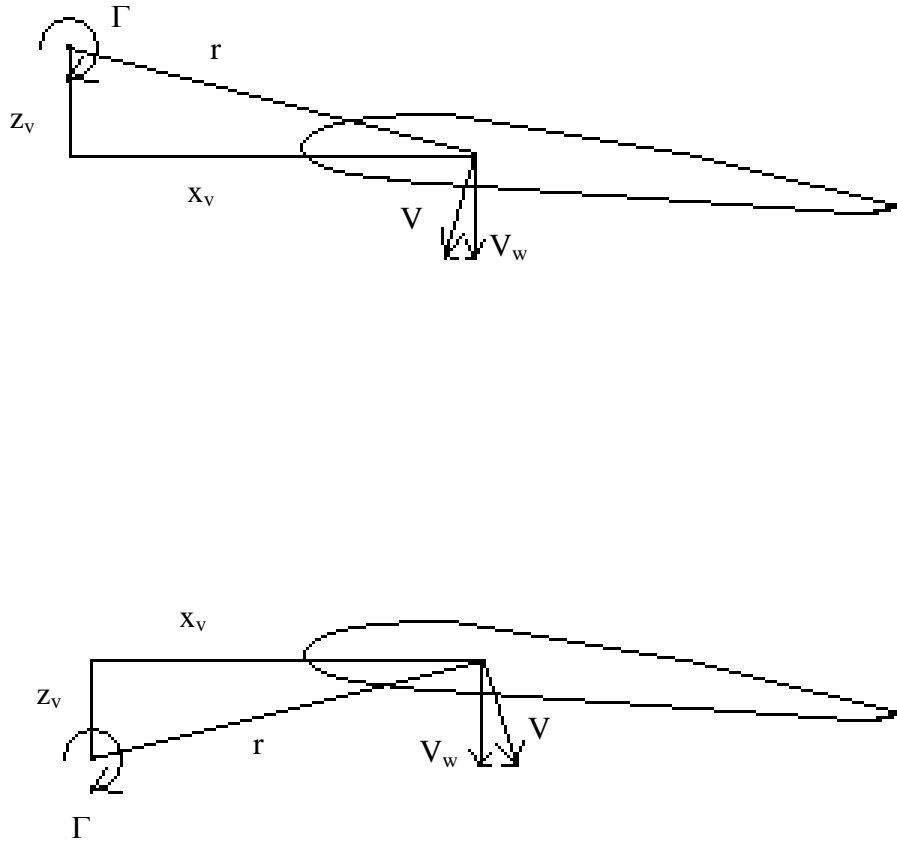
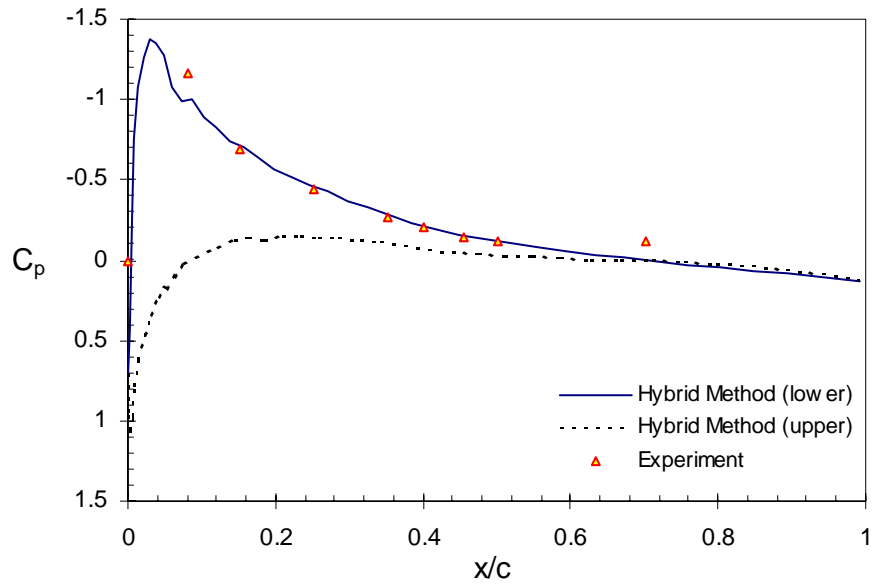


Figure 5.14: Induced Velocities by a Point Vortex above or below an Airfoil



(a) $\Psi=0^0$

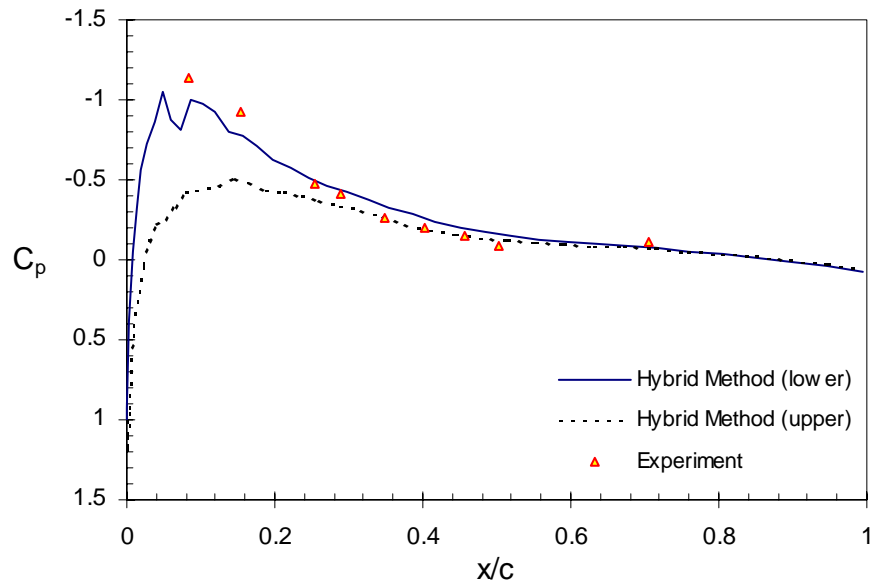
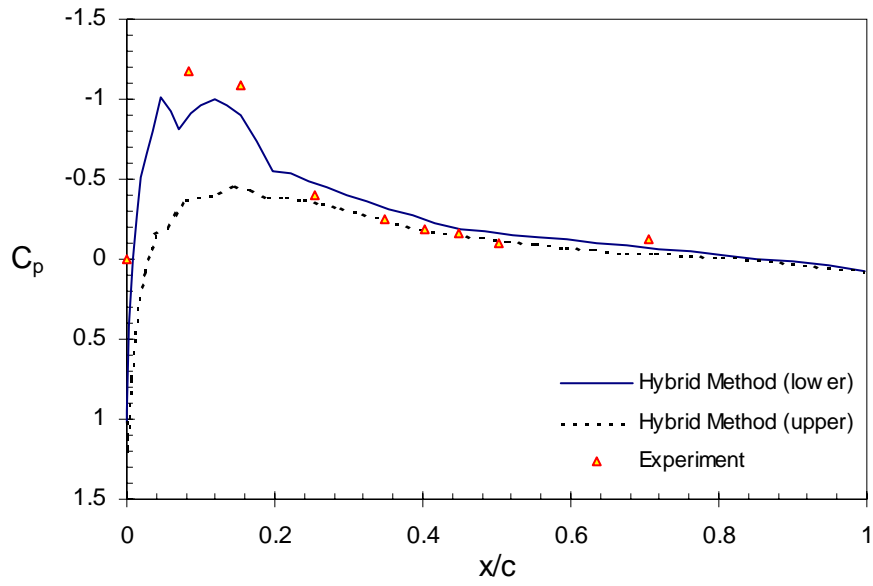


Figure 5.15: Pressure Coefficients for the OLS Rotor at $r/R=0.955$



(c) $\Psi=90^0$

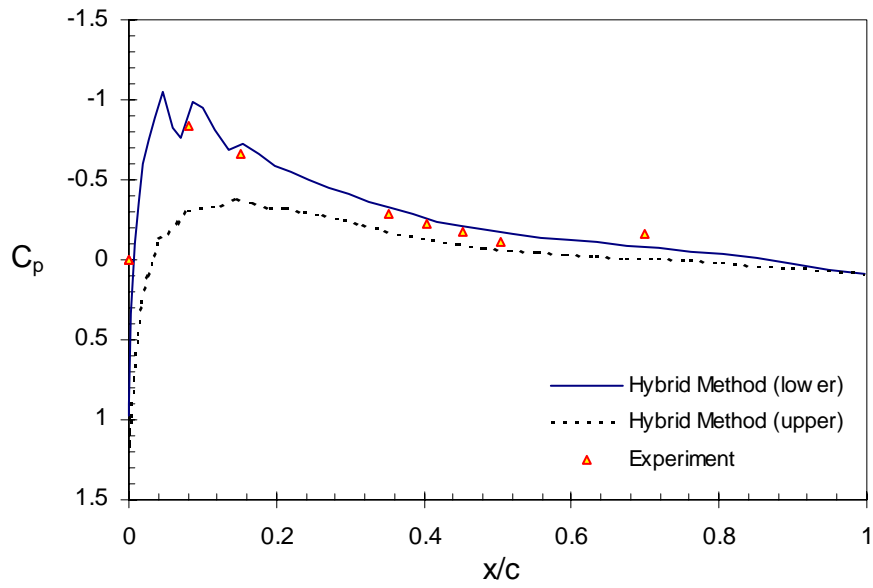


Figure 5.15: Pressure Coefficients for the OLS Rotor at $r/R=0.955$

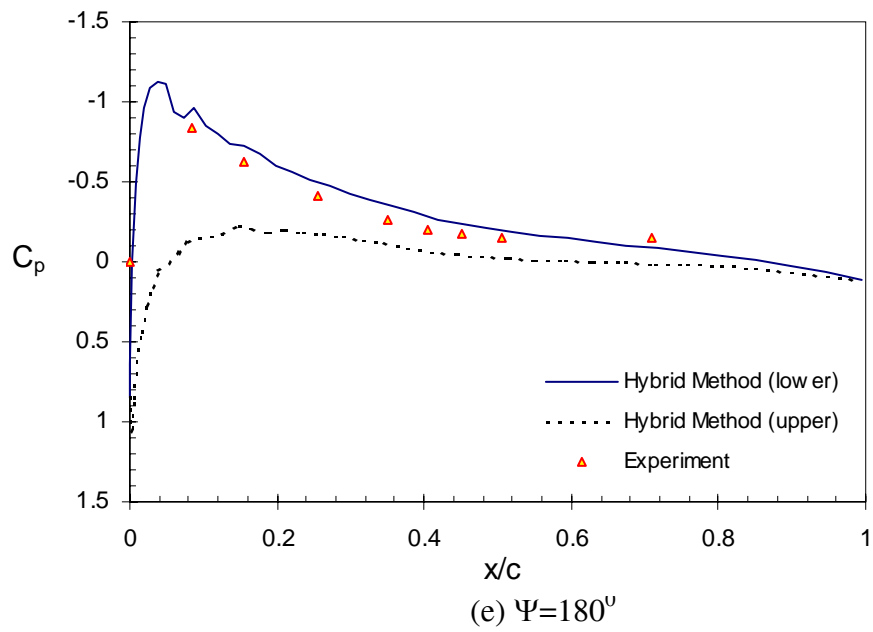


Figure 5.15: Pressure Coefficients for the OLS Rotor at $r/R=0.955$